Numerical Simulation of Plume Phenomena during Directional Solidification of Binary Alloy Calculated under Personal Computer Platform

Huang-Wen Huang[1*], Chihng-Tsung Liauh[2] and Tzyy-Leng Horng[3]

[1]Department of Software Engineering, Tamkang University Lanyang Campus, Taiwan
[2]Department of Mechanical Engineering, Kun-shan University, Tainan, Taiwan
[3]Department of Applied Mathematics, Feng Chia University, Taichung ,Taiwan

Abstract

The objective of this paper is to demonstrate the ability of simulating thermal-solute double diffusivities problem, which is usually calculated via mini-supercomputer, by using typical personal computer (PC) with optimized FORTRAN code using ALLOCATE and MODULE statements, we achieve a

phenomena due to buoyant force of lighter liquid solute during solidification will be illustrated. The conduction, convection and macrosegregation predicted by numerical simulations of a directionally solidified binary alloy (Pb-23.2 wt% Sn) are calculated on Pentium-4 1.6 GHz Personal Computer (PC) platform and presented. The casting was solidified at a rate of 6 μm s^{-1} and a thermal gradient of approximately $7.2x10^3$ Km^{-1}. The calculated results showed channels at the vertical casting surface and segregated internal pockets in the mushy zone, in agreement with the observation of freckles in experimental castings. They also showed plumes phenomena at the early stage of solidification process. The simulator ported to IBM-compatible PC platform can provide instant information on casting process for manufacturers.

Introduction

In recent years, the computational speed on PC platform has increased tremendously. It provides a convenient and instant access on predictions of scientific research and analysis. To directional solidification, it is used to cast super alloys for use as gas turbine blades. However defects have been discovered in final solidified products due to solidification processing. Ideally, the mushy zone advances vertically with planar isotherms in directional solidification (DS), and certain desirable crystalline orientations and structure can be obtained. Hence the DS process can produce high performance materials, with all the grain boundaries running in the longitudinal direction of the casting; such a microstructure enhances creep resistance by preventing failures associated with grain boundaries that are transverse to the applied stress [1]. In this apparently simple casting technique, however, localized freckles and large-scale alloy inhomogeneities may occur [2]. Such segregation is highly undesirable, because the resulting variation in physical properties within the casting can lead to expensive castings becoming scrap. The freckles are observed as long and narrow trails, aligned parallel to the direction of gravity in DS castings. Much of what

*Corresponding author, Email: hhw402@mail.tku.edu.tw

is known about freckles has been learned by studying the NH_4Cl-H_2O system solidified vertically (e.g. see Copley et al [3]. And Hellawell et al [4]). These studies demonstrated that freckles are a direct consequence of liquid plumes that emanate from channels within the mushy zone. In terms of transport phenomena, the channels are a manifestation of thermosolutal convection in a porous media (the mushy zone) subject to remelting by the interdendritic liquid laden with solute.

Table 1. Thermodynamic and transport properties used for numerical simulations.

Property	Value
Reference concentration (C_0)	23.2 wt% Sn
Reference temperature (T_0)	546.029 K
Equilibrium partition ratio (k)	0.31
Slope of liquidus (m)	-2.33K (wt%)$^{-1}$
Density [$\rho_0 = \rho(C_0, T_0)$]	1.01x10^4 kg m^{-3}
Thermal expansion coefficient (β_T)	1.2 x10^{-4} K^{-1}
Solutal expansion coefficient (β_C)	5.15x10^{-3}(wt%)$^{-1}$
Kinematic viscosity (v_0)	2.47x10^{-7}m^{2}s^{-1}
Average latent heat (L)	40 kJ kg^{-1}
Average heat capacity (c)	0.145kJ kg^{-1} K^{-1}
Average thermal diffusivity (α)	1.7x10^{-5} m^{2}s^{-1}
Solutal diffusivity (D)	2.47 x 10 $^{-7}$ m^{2}s^{-1}
Interdendritic arm spacing (d_1)	185 μm
Permeability (K_x, K_z)	

$$K_x(m^2) = \begin{cases} 1.09\times10^{-3}\phi^{3.32}d_1^{\,2} & \phi < 0.65 \\ 4.04\times10^{-6}\left(\frac{\phi}{1-\phi}\right)^{6.7336} & 0.65 \le \phi < 0.75 \\ -6.49\times10^{-2} + 5.43\times10^{-2}(1-\phi)^{0.25}d_1^{\,2} & \phi \ge 0.75 \end{cases}$$

$$K_z(m^2) = \begin{cases} 3.75\times10^{-4}\phi^{2}d_1^{\,2} & \phi < 0.65 \\ 2.05\times10^{-7}\left(\frac{\phi}{1-\phi}\right)^{10.739}d_1^{\,2} & 0.65 \le \phi < 0.75 \\ 0.074[\log(1-\phi) - 1.49 + 2(1-\phi) - 0.5(1-\phi)^2]d_1^{\,2} & \phi \ge 0.75 \end{cases}$$

There has been much work on using porous media theory to simulate thermosolutal convection, macrosegregation, and freckles in binary alloys numerically [5-11]. The solidification of multicomponent solutions illustrates a general transport problem, which is applicable to a diversity of scientific disciplines [12, 13]. Solidification involves complex interactions of heat and mass transfer, fluid flow, phase change, and sometimes chemical reactions. Additionally, solidification processes occur on both microscopic and macroscopic scales [14]. Because of the complex coupling of the various physical processes and the opacity of materials, solidification is inherently difficult to study experimentally or theoretically, yet there is the need to predict transport phenomena and their effects on the quality of cast materials accurately.

The present study is concerned with obtaining an improved understanding of the transport phenomena in the documented experiments of Tewari and Shah [15], who employed rather steep thermal gradients of approximately 70 to 100 K cm^{-1} during vertical directional solidification of Pb-Sn alloys. In our previous work and in that of others, the simulation of the DS process with such steep gradients was not attemped. Tewari and Shah reported macrosegregation along the length of a small diameter (7mm) rod of Pb-Sn alloys (10 to 58 % Sn) when it was directionally solidified in a strong positive thermal gradient (melt on top, solid below, and gravity pointing downwards). The results presented here are numerical simulations of the convection and segregation in the directionally solidified Pb-23.2 wt%Sn alloy, using the thermal conditions specified by Tewari and Shah.

With a finite element simulator, the

*Corresponding author, Email: hhw402@mail.tku.edu.tw

solidification process is modelled by solving the fully coupled equations of momentum, energy, and solute transport, along with the constraint of assuming local equilibrium on the complex solid-liquid interface in the mushy zone. The simulations are based on a mathematical model [7, 11, 16, 17] of dendritic solidification, in which the mushy zone is treated as an anisotropic poros medium of variable porosity. The alloy solidifies vertically from the bottom of a rectangular container.

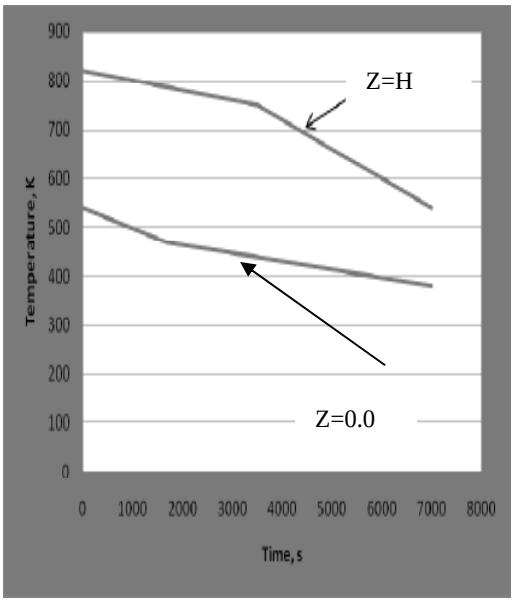

Figure 1. Temperature versus time in the directionally solidified Pb-23.2 wt%Sn alloy.

Although Tewari and Shah solidified alloys in the form of circular cylinders, our simulations are in two-dimensional rectangular coordinates. We accept, therefore, that the simulations do not capture the full three-dimentional convection patterns in the experimental alloys. The calculated results, however, are robust enough to show channels located at the surface of the casting walls and segregated internal pockets in the mushy zone of the solidifying alloy, in agreement with the observation of freckles in the experimental casting [15]. Simulated results at different times are presented to show the unstable nature of the convection cells and the development of the channels in the mushy zone.

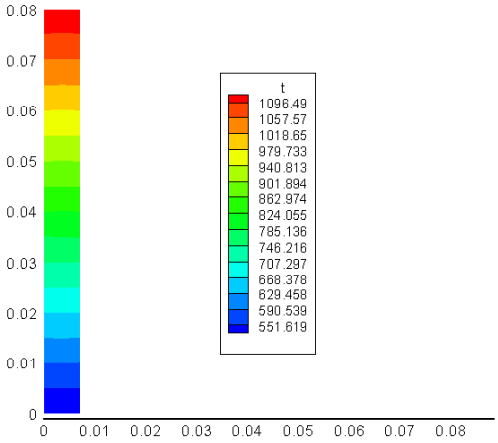

Figure 2. Temperature distribution at 1000 s. (K)

Boundary conditions and problem specification

In this work, we are concerned with Pb-23.2 wt%Sn alloy, with the thermodynamic and transport properties given in Table 1. The liquidus and solidus lines are approximated as straight lines with negative slopes, and the temperature is related to the concentration of Sn in the liquid in the mushy zone, C_l, by $T = T_M + mC_t$, where T_M is the melting point of pure lead and m is the slope of liquidus line. The molten alloy is in a rectangular domain with a width W = 7 mm and height H = 40 mm.

The primary dendrite arm spacing used in the simulations was 185 μm, taken from the experiment of Tewari and Shah [15]. With dendritic columnar grains, the permeability is anisotropic with components K_x and K_z for flow perpendicular and parallel to the columnar dendrites, respectively; K_x and K_z depend on the primary dendrite arm spacing and fraction liquid and were deduced from [18] and

*Corresponding author, Email: hhw402@mail.tku.edu.tw

[19]. In the former, permeabilities based on empirical measurements for $g_L < 0.65$ are reported. Since there are no empirical data for $g_L > 0.65$, estimates of the permeability were made by regressing calculated permeabilities for flow parallel to primary dendrite arms and for flow perpendicular to cylinders, to approximate primary dendrite arms. (g_L is fraction of liquid)

The temperature at the top (z = H) and bottom (z = 0) surfaces are specified as functions of time that were derived from the thermal profiles measured by Tewari and Shah [15]. In their experiments, the directionally solidified alloys were fixed and the furnace was withdrawn upwards at a constant rate. A thermocouple in the alloy provided temperature versus time, and this was transformed to a plot of temperature versus distance. The transformation could be made because the furnace was withdrawn at a constant rate, and the speed of the isotherms was equal to the speed of the furnace. For our calculations, we transformed their thermal data to give temperature versus time at z = 0 and z = H (Figure 1). In a simulation, the initial condition is a nonconvecting melt of uniform composition with a linear temperature distribution from the bottom to top corresponding to t = 0 in Figure 1. Both side walls are thermally insulated, and the bottom surface and the two side walls are impermeable to all mass and solute fluxes. As an approximation, the top surface (z = H) is treated as a stress-free surface to allow for flow across that surface, or equivalently the container has an indefinite height.

In the experimental setup, the length of the melt column was approximately 120 mm. The reasons for using 40 mm as the length of the domain in the numerical simulation are the limitation of computational speed and the three zones comprising liquid at the top, an intermediate mushy zone, and all solid at the bottom can be achieved in the 40 mm. Also, the directional solidification was sustained in a steady state manner.

Mathematic model

The focus of the numerical modeling in this study is on the macroscopic details associated with a solidifying binary alloy. Several numerical modeling techniques concerning solidification have been proposed in the past two decades. Some techniques are based on the multiple domain approach, in which the all-liquid, mushy zone, and all-liquid regions are treated separately but coupled through interface conditions. This approach is difficult to implement numerically, because the interfaces of solidus and the liquidus must be tracked as functions of time as solidification proceeds. In contrast, in single region or continuum models, a system of equations is developed through the application of either volume averaging or mixture theory. The equations are valid throughout the domain, regardless of the particular region under consideration. Examples of the latter type of models include Bennon and Incropera [20], Beckermann and Viskanta [6], and Felicelli et al [7, 11].

The equations of conservation of mass, momentum, energy and solute content are solved by finite element method, using Petro-Galerkin formulation [11, 21] in the two-dimensional domain under the following assumptions:

1. The flow is laminar.
2. Only solid and liquid phases are present, i.e., No pores form.
3. The solid and liquid phases have equal densities.
4. The density is constant except in the buoyancy term of momentum equations.

*Corresponding author, Email: hhw402@mail.tku.edu.tw

5. No diffusion of solute within the solid.
6. The solid does not convect.
7. The thermal properties are constant and equal in both the liquid and solid phases.

Based on the these assumptions, the mass conservation equation is

$$\frac{\partial u}{\partial x}+\frac{\partial w}{\partial z}=0 \qquad (1)$$

Where u and w are the components of the superficial velocity (i.e. the volume fraction liquid times the interdendritic velocity) in the x and z directions. The component equations for momentum are:

(x momentum)

$$\frac{\partial u}{\partial t}+\frac{u}{\phi}\frac{\partial u}{\partial x}+\frac{w}{\phi}\frac{\partial u}{\partial z}=-\frac{\phi}{\rho_0}\frac{\partial P}{\partial x}+\upsilon_0\left(\frac{\partial^2 u}{\partial x^2}+\frac{\partial^2 u}{\partial z^2}\right)-\frac{\upsilon_0\phi}{K_x}u \qquad (2)$$

(z momentum)

$$\frac{\partial w}{\partial t}+\frac{u}{\phi}\frac{\partial w}{\partial x}+\frac{w}{\phi}\frac{\partial w}{\partial z}=-\frac{\phi}{\rho_0}\frac{\partial P}{\partial z}+\upsilon_0\left(\frac{\partial^2 w}{\partial x^2}+\frac{\partial^2 w}{\partial z^2}\right)-\frac{\upsilon_0\phi}{K_z}w-\phi\frac{\rho}{\rho_0}g \qquad (3)$$

Where t is time, P is pressure, υ_0 is the kinematic viscosity, ρ_0 is the density at the reference state, and g is the gravitational acceleration pointing down in the negative direction. K_x and K_z, the components of the permeability, and ϕ, volume fraction liquid, are the variables that connect the microstructural aspects of dendritic mushy zone to the convection and solute redistribution in the macroscopic domain. The density, ρ, in the equation (3) is assumed to be a linear function of the temperature, T, and the solute concentration of the liquid, C_l; hence,

$$\rho=\rho_0\left[1-\beta_T\left(T-T_0\right)-\beta_C\left(C_l-C_0\right)\right] \qquad (4)$$

where β_T is the thermal expansion coefficient and β_C is the solutal expansion coefficient. For the reference state, the concentration is that of the initial melt (C_0) and the temperature is the liquidus temperature (T_0) corresponding to C_0 on the equilibrium phase diagram.

The energy equation is

$$\frac{\partial T}{\partial t}+u\frac{\partial T}{\partial x}+w\frac{\partial T}{\partial z}=\alpha\left(\frac{\partial^2 T}{\partial x^2}+\frac{\partial^2 T}{\partial z^2}\right)-\frac{L}{c}\frac{\partial\phi}{\partial t} \qquad (5)$$

where α is the thermal diffusivity, c is the heat capacity of the solid and L is the latent heat of fusion. The latent heat of fusion is assumed to be constant in equation (5).

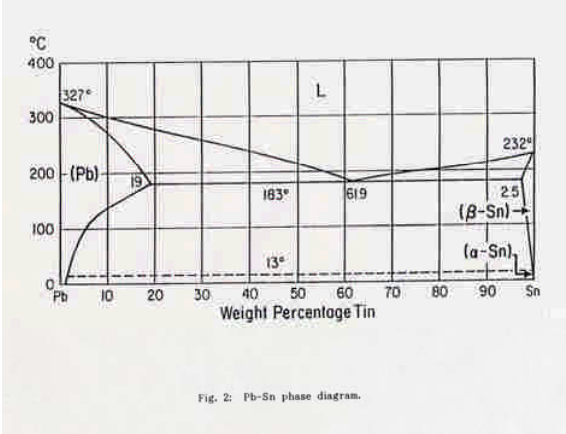

Fig. 2: Pb-Sn phase diagram.

Figure 2.1 Pb-Sn phase diagram

The conservation of solute mass in a volume element during solidification is

$$\frac{\partial\bar{C}}{\partial t}+u\frac{\partial C_l}{\partial x}+w\frac{\partial C_l}{\partial z}=D\left\{\frac{\partial}{\partial x}\left(\phi\frac{\partial C_l}{\partial x}\right)+\frac{\partial}{\partial z}\left(\phi\frac{\partial C_l}{\partial z}\right)\right\} \qquad (6)$$

where D is the solutal diffusivity (assumed to be uniform) and $\bar{C}$ is the total average concentration in liquid and solid together. That is

$$\bar{C}=\phi C_l+(1-\phi)\bar{C}_s \qquad (7)$$

and $\bar{C}_s$ is the average local concentration in the solid.

In dendritically solidifying binary alloys, the composition of the interdendritic liquid at a given temperature is uniform, and the local solid-liquid interface is effectively at equilibrium. Hence, the composition of the interdendritic liquid is given by

*Corresponding author, Email: hhw402@mail.tku.edu.tw

the liquidus line in the phase diagram (**Figure** 2.1) of the alloy: that is, $C_l = C_L(T)$. In the all-liquid zone, however, $C_l = \bar{C}$ resulting from diffusion and convection, according to equation (6). Hence,

$$C_l = \begin{cases} C_L(T) & \text{if } \phi < 1 \\ \bar{C} & \text{if } \phi = 1 \end{cases} \quad (8)$$

Noted that if $\phi < 1$, $C_l = C_L(T)$ is at liquidus line in the phase diagram. In modeling the composition of solid, C_s, microsegregation is allowed by assuming that there is no diffusion in the solid. Therefore, C_s is not uniform within a solidifying element. Rather, the average composition of solid, $\bar{C}_s$, is

$$\bar{C}_s = \frac{1}{1-\phi}\int_{\phi}^{1} kC_l \, d\phi \quad (9)$$

where k is the equilibrium partition ratio, defined as the ratio of the concentration of solute at dendritic-solid interface to the concentration of solute in the interdendritic liquid.

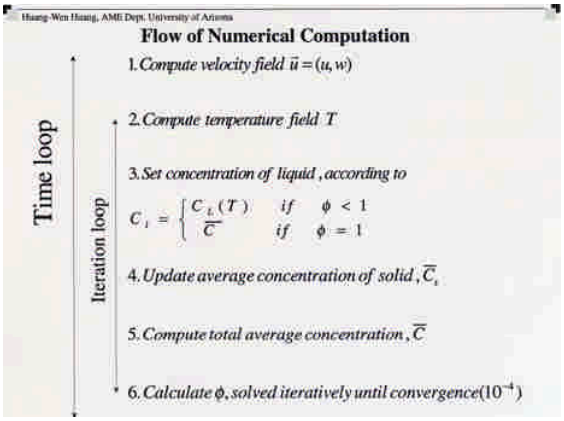

Figure 2.2 Flow of numerical computation

It is possible that remelting and channeling occur in the mushy zone during solidification. As expected by Felicelli et al [7], this requires that the average composition of the solid must be taken from the solidification history at every node in the mesh.

The flow of numerical computation using finite element method based on mathematical equations of thermal, momentum and solute is shown in figure 2.2.

Results

The computational domain was discretized with a uniform mesh of 30 elements in x direction (horizontal) and 80 elements in z direction (vertical). This mesh was selected after several preliminary calculations were performed with different resolutions to assess the sensitivity of the results to the mesh size.

In this work, the thermal gradients during solidification are much higher than we or anyone else have numerically simulated before [7-11], so that relatively small time steps and a fine mesh had to be used. In order to save CPU time a nondimensional velocity magnitude of 10^{-6} was assigned as an indicator to determine whether convection in the solute transport process should be discounted. Even so, every 1000 s of real time took about 20 hours of CPU time on Convex C240 minisuper computer. With optimized FORTRAN code using ALLOCATE and MODULE statements on PC, we achieve a much less CPU time consumed in PC.

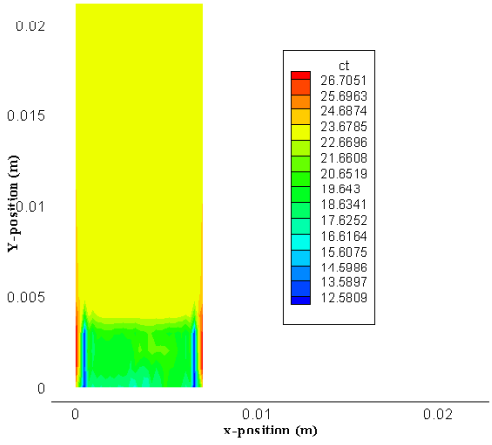

*Corresponding author, Email: hhw402@mail.tku.edu.tw

Figure 3. Solute concentration at 1000 s, wt% Sn, with a height 0f 2 cm

The initial melt with 23.2 wt% Sn is solidified from the bottom with a steep thermal gradient of 77 K cm^{-1} near the tips of the dendrites and the temperature specified by Figure 1. With such a high temperature gradient (Figure 2), the numerical modeling is more difficult than with a low temperature gradient. The most critical aspects involved in a successful calculation are the following: 1) Once the mushy zone begins to develop, the solute concentration in the liquid is calculated from the phase diagram. This creates a solute flux through the bottom boundary unless special precautious are taken to ensure that the mass flux of solute concentration in the liquid is zero at the bottom. 2) Channels enclosed by fully solidified material may form. One must ensure that as those channels solidified, gradients of the solute concentration in the liquid are not allowed. Otherwise this causes a numerical instability and/or unrealistic results. 3) The model is sensitive to the way in which the end of the solidification process is handled. In the present calculations, we have used the criterion that solidification is complete when the volume fraction of interdendritic liquid is less than one percent. This can happen at or before the eutectic temperature is reached.

The results are given as a series of figures that illustrate the complex transport phenomena and structure development during directional solidification. The reader should keep in mind that we have intentionally selected an experimental case in which the thermal conditions led to freckles and obvious macrosegregation.

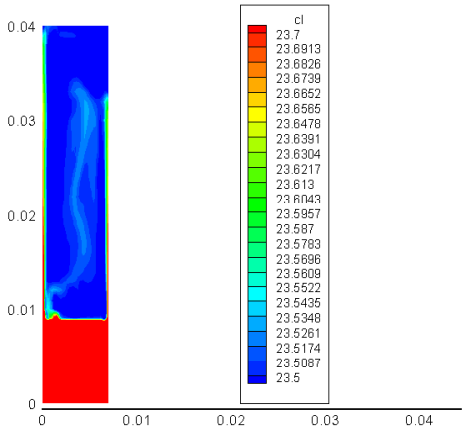

Figure 4. Liquid solute concentration at 2000 s. Colour code restricted to 23.5 <=C_L<=23.7 wt% Sn.

After 1000 s, the concentration is no longer uniform (Figure 3), and the mushy zone has advanced about 6 mm but is not yet completely formed. Already there is positive segregation (~30 wt% Sn) at both walls and in several pockets within the mushy zone and to the left of the centre. Near each side wall, the liquid advects solute upwards to the overlying liquid. The thermosolutal convection also

wall. The pocket and plume can be better seen in figure 4, where the concentration field in the range from 23.5 to 23.7 wt% Sn was adopted in selecting the colours.

From the distribution of the fraction of liquid in the computational domain, the overall shape of the mushy zone is irregular because of the extensive along thermosolutal convection, and we can observe clearly the channels that are developing along the walls.

In order to describe the convection, the stream function is analyzed. The stream function at 1000 sec is (-2.615~3.541)x10^{-6} m^2s^{-1}. It shows convection as four strong cells just above the dendrite tips. When

*Corresponding author, Email: hhw402@mail.tku.edu.tw

viewing the stream function in the range of (-3.341~3.341)x10^{-8} m^2s^{-1}, it brings out the weak convection within the mushy zone. Weak as it is, however the speed is comparable to the speed of isotherms so that the advection of the solute is an important ingredient of the total redistribution of solute in the mushy zone. It also shows penetration of the liquid zone into mushy zone and how the liquid circulates and moves towards the side walls.

Through this simulation at 4000 sec, it shows macrosegregation, volume fraction liquid, and channels in the mushy zone. Several important features can be observed, and they compare well to experimental results. There are long narrow segregates aligned parallel to gravity which are enriched in the normally segregating elements and depleted of the inversely segregating elements, and segregated channels with rich solute content at the side walls. It also indicates that the internal liquid pocket located at 5 mm from the bottom near center area, which corresponds to the initialization of packet at 1000 s in figures 3-4. This is convincing evidence of remelting within the mushy zone during solidification that led to the long channel that eventually meandered somewhat to the right and then turn to the left. The result also shows the volume fraction of liquid across the casting after 4000s; we see that the overall structure of the mushy zone is complex.

Flemings [22] gives the condition for remelting: it is:

$$\frac{V \bullet \nabla T}{\varepsilon} < -1 \qquad (10)$$

Where V is the velocity of fluid flow, ∇T is the temperature gradient, and ε is the local rate of temperature change. The meaning behind equation (10) is simply that when the speed of the interdendritic liquid exceeds the isotherm speed in the same direction, then there is remelting. This was verified by examining the numerical output in the simulation presented as Figure 5.

The simulations presented here using PC (Personal Computer) are the same as those calculations under mini-super computer and in a good agreement with experiments. Numerical study shows stream function after 4000s of solidification, and it give a clear illustration that strong convection is near and above the tip of dendrites.

At the present study, the assumption of same solid and liquid densities of alloy is used, although it is not the case in real application. But the convection generated due to density variation is limited and can be found in the study of [23].

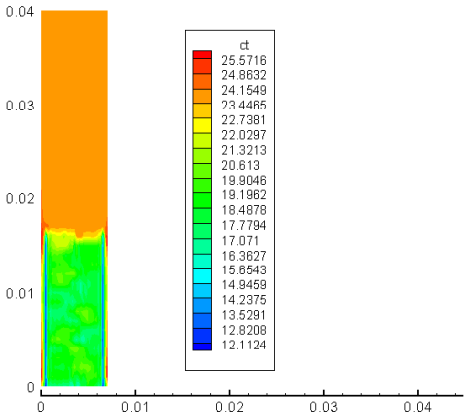

Figure 5. Solute concentration at 4000 s, wt% Sn.

References

[1] The Metals Society) pp 1-8 (1983)

[2] Giamei A F and Kear B H, Metall. Trans., **1** 2185 (1970).

[3] Copley S M, Giamei A F, Johnson S M and

*Corresponding author, Email: hhw402@mail.tku.edu.tw

Hornbecker M F, Metall. Trans. **1** 2193(1970).

[4] Hellawell A, Sarazin J R and Steube R S, Phil. Trans. R. Soc. Land. 345A 507 (1993).

[5] Bennon W D and Incropera F P, Metall. Trans. **18B** 611 (1987).

[6] Beckermann C and Viskanta R , Phys. Chem. Hydrodyn. **10** 195 (1988).

[7] Felicelli S D, Heinrich J C and Poirier D R, Metall. Trans. **22B** 847 (1991).

[8]

solidification of a binary model alloy and the

DOE/ER/13759-5, U.S.A. (1992).

[9]

Casting, Welding and Advanced Solidification Processes

Katgerman (Warrendale, PA: The Minerals, Metals and Materials Society) pp 227-34(1993).

[10]

Casting, Welding and Advanced Solidification Processes

L Katgerman (Warrendale, PA: The Minerals, Metals and Materials Society) pp 201-8 (1993).

[11] Heinrich J C, Felicelli S D and Poirier D R, Comp. Meth. Appl. Meth. Eng. **89** 435 (1991).

[12] Turner J S, Ann. Rev. Fluid Mech. **6** 37 (1974).

[13] Huppert H E, J. Fluid Mech. **212** 209 (1990).

[14]

and Advanced Solidifica

S Piwonka, V Voller and L Kagerman (Warrendale, PA: The Minerals, Metals and Materials Society), pp 181-92 (1993).

[15] Tewari S N and Shah R, Metall. Trans. 23A 3383 (1992).

[16] Ganesan S, Chan C L and Poirier D R, Mater. Sci. Eng. A 151 97 (1992).

[17] Poirier D R, Nandapurkar P J and Ganesan S, Metall. Trans. 22B 889 (1991).

[18] Poirier D R, Metall. Trans. B 19 245 (1987).

[19] Ganesan S, Chan C L and Poirier D R, Mater. Sci. Eng. A 151 97 (1992).

[20] Bennon W D and Incropera F P, Int. J. Heat Mass Transfer 30 2161 (1987).

[21] Felicelli S D, Heinrich J C and Poirier D R, Num. Heat Transfer B 23 461 (1993).

[22]

ill) pp 249-51 (1974).

[23] E. McBride, J.C. Heinrich and D.R. Poirier: "Numerical Simulation of Incompressible Flow Driven by Density Variations during Phase Change," Inter. J. Num. Meth. Fluids, vol. 31, 1999, pp. 787-800.

*Corresponding author, Email: hhw402@mail.tku.edu.tw